

## Catalytic Proficiency of Ubiquitin Conjugation Enzymes: Balancing $pK_a$ Suppression, Entropy, and Electrostatics

Craig J. Markin,<sup>†</sup> Linda F. Saltibus,<sup>†</sup> Melissa J. Kean,<sup>†</sup> Ryan T. McKay,<sup>‡</sup> Wei Xiao,<sup>§</sup>  
and Leo Spyropoulos<sup>\*†</sup>

*Department of Biochemistry, School of Molecular and Systems Medicine, University of Alberta, Edmonton, Alberta T6G 2H7, Canada, National High Field Nuclear Magnetic Resonance Center (NANUC), University of Alberta, Edmonton, Alberta T6G 2H7, Canada, and Department of Microbiology and Immunology, University of Saskatchewan, Saskatoon, Saskatchewan, S7N 5E5, Canada*

Received June 16, 2010; E-mail: leo.spyropoulos@ualberta.ca

**Abstract:** Biological organisms orchestrate coordinated responses to external stimuli through temporal fluctuations in protein–protein interaction networks using molecular mechanisms such as the synthesis and recognition of polyubiquitin (polyUb) chains on signaling adaptor proteins. One of the pivotal chemical steps in ubiquitination involves reaction of a lysine amino group with a thioester group on an activated E2, or ubiquitin conjugation enzyme, to form an amide bond between Ub and a target protein. In this study, we demonstrate a nominal 14-fold range for the rate of the chemical step,  $k_{cat}$ , catalyzed by different E2 enzymes using non-steady-state, single-turnover assays. However, the observed range for  $k_{cat}$  is as large as  $\sim 100$ -fold for steady-state, single-turnover assays. Biochemical assays were used in combination with measurement of the underlying protein–protein interaction kinetics using NMR line-shape and ZZ-exchange analyses to determine the rate of polyUb chain synthesis catalyzed by the heterodimeric E2 enzyme Ubc13–Mms2. Modest variations in substrate affinity and  $k_{cat}$  can achieve functional diversity in E2 mechanism, thereby influencing the biological outcomes of polyubiquitination. E2 enzymes achieve reaction rate enhancements through electrostatic effects such as suppression of substrate lysine  $pK_a$  and stabilization of transition states by the preorganized, polar enzyme active site as well as the entropic effects of binding. Importantly, modestly proficient enzymes such as E2s maintain the ability to tune reaction rates; this may confer a biological advantage for achieving specificity in the diverse cellular roles for which these enzymes are involved.

### Introduction

Biological organisms orchestrate exquisite responses to various stimuli through temporal fluctuations in protein–protein interaction networks. The ebb and flow of information within these networks is central to life processes, encompassing diverse roles such as repair of damaged DNA<sup>1</sup> and innate immune responses to bacterial pathogens.<sup>2</sup> A key crossroad in such pathways involves the build up and recognition of polyubiquitin (polyUb) chains on adaptor proteins.<sup>3</sup> Ubiquitination is realized through the combined catalytic activity of an enzyme cascade that is initiated by covalent attachment of the C-terminus of Ub (Gly76) to the active site cysteine of a Ub activating enzyme (E1), followed by transfer as a thioester conjugate to a Ub conjugating enzyme (E2). Ultimately, Ub is attached to target proteins through the action of a ubiquitin ligase (E3) which binds the E2 enzyme and the target to facilitate nucleophilic attack of the amino group from a substrate lysine on the thioester bond

between the C-terminus of Ub and the conserved cysteine within the E2 active site.<sup>4</sup>

The diversity of the molecular architecture for the Ub signal is abundant, extending well beyond the archetypal K48-linked polyUb chain, which destines proteins for degradation. Numerous topological variants of the Ub signal have been identified, such as attachment of a single, or multiple Ub molecules to different target protein sites, or polyubiquitination through single or variable Ub peptide bonds.<sup>3</sup> This wide topological variety for the Ub signal likely imparts organisms with a biological advantage for achieving specificity in diverse signaling cascades.

The first step of the ubiquitination cascade, catalyzed by E1 enzyme, is the only one requiring energy through hydrolysis of ATP. The multiple steps in the kinetics of the reaction catalyzed by E1 enzyme are characterized by a turnover number of 1–2  $s^{-1}$ .<sup>5</sup> In contrast, the catalytic rate for conjugation of Ub to substrates or build up of polyUb chains is substantially slower, with apparent  $k_{cat}$  values ranging from 0.01 to 0.1  $s^{-1}$ .<sup>6,7</sup> This 10-fold variability in apparent rates combined with differences

<sup>†</sup> Department of Biochemistry, School of Molecular and Systems Medicine, University of Alberta.

<sup>‡</sup> National High Field Nuclear Magnetic Resonance Center, University of Alberta.

<sup>§</sup> University of Saskatchewan.

(1) Petrini, J. H. J. *Science* **2007**, *316*, 1138–1139.

(2) Covert, M. W.; Leung, T. H.; Gaston, J. E.; Baltimore, D. *Science* **2005**, *309*, 1854–1857.

(3) Komander, D. *Biochem. Soc. Trans.* **2009**, *37*, 937–953.

(4) Glickman, M. H.; Ciechanover, A. *Physiol. Rev.* **2002**, *82*, 373–428.

(5) Haas, A. L.; Rose, I. A. *J. Biol. Chem.* **1982**, *257*, 10329–10337.

(6) Pickart, C. M.; Eddins, M. J. *Biochim. Biophys. Acta* **2004**, *1695*, 55–72.

(7) Haas, A. L.; Bright, P. M.; Jackson, V. E. *J. Biol. Chem.* **1988**, *263*, 13268–13275.

in substrate binding ( $K_M$ ) suggest a functional diversity in the E2 mechanism that may be important in achieving specificity for the various biological reactions regulated by ubiquitination.<sup>7</sup> Indeed, it has recently been demonstrated that attachment of Lys48-linked polyUb to substrates derived from  $\beta$ -catenin and cyclin E1 proteins by their cognate E2–E3 pairs Cdc34–SCF<sup>Cdc34</sup> and Cdc34–SCF <sup>$\beta$ -TrCP</sup>, respectively, occurs through sequential addition of Ub molecules to substrate.<sup>8</sup> Importantly, a 10-fold difference in the overall rate at which the first Ub molecule was attached to the different substrates was observed. Within the context of a sequentially processive kinetic model, that is, sequential addition of Ub molecules to a substrate,<sup>8</sup> a small rate difference for the attachment of the first Ub molecule leads to a significant difference in the fraction of substrates bearing chains of four Ubs, the minimum required for degradation by the proteasome. As interesting as this kinetic diversity appears, it remains a problem to develop a molecular mechanism for this key regulatory process in ubiquitination.

The rate for covalent attachment of the first Ub to a substrate depends on the catalytic proficiency of E2 enzymes or ( $k_{cat}/K_M$ )/ $k_{noncat}$ . The magnitude of the catalytic proficiency ranges from  $10^8$  to  $10^{23} \text{ M}^{-1}$  and is indicative of the ability of a given enzyme to produce a large rate enhancement ( $k_{cat}/k_{noncat}$ ). Alternatively stated, it is the degree to which an enzyme reduces the activation barrier for a reaction in comparison to the reaction in water.<sup>9,10</sup> In comparison, the efficiency of an enzyme ( $k_{cat}/K_M$ ) has a maximum value equal to the diffusion limit ( $\sim 10^9 \text{ M}^{-1} \text{ s}^{-1}$ ) and represents the efficiency of catalysis with respect to substrate binding. Thus, variability in either  $k_{cat}$  or  $K_M$  among E2 enzymes represents a regulatory mechanism for polyubiquitination of substrate proteins and the ensuing biological outcomes. The central problem, therefore, is to understand the chemical mechanism for ubiquitination within the context of the catalytic proficiency of E2 enzymes. Kinetic studies of nucleophilic addition of ammonia to thioesters in water using model compounds<sup>11</sup> can be used to calculate a noncatalyzed rate ( $k_{noncat}$ ), giving a rate enhancement  $k_{cat}/k_{noncat} \approx 10^6$ – $10^9$ . Thus, the catalytic proficiency of E2 enzymes is modest, with ( $k_{cat}/K_M$ )/ $k_{noncat} \approx 10^{11}$ – $10^{14} \text{ M}^{-1}$ .<sup>10</sup> In comparison, the most proficient enzyme is OMP decarboxylase, with a catalytic proficiency of  $2 \times 10^{23} \text{ M}^{-1}$ , and the least proficient enzyme is cyclophilin with a catalytic proficiency of  $5 \times 10^8 \text{ M}^{-1}$ .<sup>9</sup>

Recently, for the biological reaction involving attachment of the Ub-like modifier SUMO to the protein substrate GST-RanGAP1 catalyzed by the E2 Ubc9, the catalytic rate enhancement was attributed to a downshift of the  $pK_a$  of the substrate lysine ( $\Delta pK_a \approx -4$ ), arising from desolvation effects within the active site.<sup>12</sup> That is, the active site environment favors deprotonation of the substrate lysine to promote nucleophilic attack on the thioester bond. This type of catalytic enhancement was proposed on the basis of the pH–rate profile for the acylation of acetoacetate decarboxylase.<sup>13</sup> However, lysine  $pK_a$  suppression may not be the sole source of the catalytic power of E2 enzymes, given that 3–4  $\Delta pK_a$  units correspond to a rate enhancement of 1000 to 10 000 fold. In addition, the emerging view from computational studies of enzyme mechanism indi-

cates that the main source of catalytic power for many enzymes is stabilization of transition states by electrostatic complementarity.<sup>14,15</sup> In this regard, the entropic effects of binding were considered to be a major mechanism by which enzymes achieve large rate enhancements.<sup>16</sup> However, computational studies indicate that these entropic effects are much smaller than previously suggested.<sup>17</sup>

In this study, we performed enzyme assays to measure non-steady-state kinetics for assembly of Lys63-linked polyUb chains catalyzed by the heterodimeric enzyme Mms2–Ubc13. Lys63-linked polyUb chains are critical for recruiting DNA polymerases to the sliding clamp PCNA, thereby initiating error-free postreplicative DNA repair.<sup>18–20</sup> Lys63-linked chains play key roles in the immune response through polyubiquitination of the signaling adapter protein TRAF6 and ultimately result in altered gene expression by activation of the transcription factor NF- $\kappa$ B.<sup>21</sup> These chains are also essential for recruitment of DNA repair protein complexes to sites of DNA double-strand breaks.<sup>22–24</sup>

The heterodimeric enzyme Mms2–Ubc13 is composed of the E2 Ubc13, which contains a catalytic cysteine, and Mms2, an E2-like protein that is structurally similar to Ubc13 but lacks a catalytic cysteine. For Ubc13, E1 enzyme catalyzes the covalent attachment of the C-terminus of a “donor” Ub to the catalytic cysteine through a thioester bond. Mms2 is tightly bound to Ubc13 and binds an “acceptor” Ub such that Lys63 is proximal to the thioester bond of the catalytic cysteine from Ubc13, facilitating nucleophilic attack of the acceptor Ub on the thioester bond of the donor Ub.<sup>25,26</sup> In general,  $k_{cat}$  and  $K_M$  values for E2 enzymes are determined using initial rate analysis under the assumption of steady-state, Michaelis–Menten kinetics. However, E2-catalyzed reactions are strictly non-steady state, given that E2 enzyme with a thioester-conjugated Ub molecule is consumed during the reaction with substrate. Furthermore, the noncovalent interaction between Mms2 and Ubc13 is not accounted for in the basic Michaelis–Menten enzymatic reaction. Thus, we derived rate laws to describe the non-steady-state kinetics for catalysis of polyUb chains by Mms2–Ubc13, which included the kinetics of the various protein–protein interactions involved in the mechanism. The protein–protein interaction kinetics were characterized using NMR line-shape and ZZ-exchange analyses. The results indicate that different E2s have 10- to 100-fold variability in rate

(8) Pierce, N. W.; Kleiger, G.; Shan, S. O.; Deshaies, R. J. *Nature* **2009**, *462*, 615–619.

(9) Radzicka, A.; Wolfenden, R. *Science* **1995**, *267*, 90–93.

(10) Wolfenden, R.; Snider, M. J. *Acc. Chem. Res.* **2001**, *34*, 938–945.

(11) Connors, K. A.; Bender, M. L. *J. Org. Chem.* **1961**, *26*, 2498–2504.

(12) Yunus, A. A.; Lima, C. D. *Nat. Struct. Mol. Biol.* **2006**, *13*, 491–499.

(13) Schmidt, D. E.; Westheimer, F. H. *Biochemistry* **1971**, *10*, 1249–1253.

(14) Villa, J.; Warshel, A. *J. Phys. Chem. B* **2001**, *105*, 7887–7907.

(15) Garcia-Viloca, M.; Gao, J.; Karplus, M.; Truhlar, D. G. *Science* **2004**, *303*, 186–195.

(16) Page, M. I.; Jencks, W. P. *Proc. Natl. Acad. Sci. U.S.A.* **1971**, *68*, 1678–1683.

(17) Villa, J.; Strajbl, M.; Glennon, T. M.; Sham, Y. Y.; Chu, Z. T.; Warshel, A. *Proc. Natl. Acad. Sci. U.S.A.* **2000**, *97*, 11899–11904.

(18) Xiao, W.; Lin, S. L.; Broomfield, S.; Chow, B. L.; Wei, Y. F. *Nucleic Acids. Res.* **1998**, *26*, 3908–3914.

(19) Hofmann, R. M.; Pickart, C. M. *Cell* **1999**, *96*, 645–653.

(20) Hoege, C.; Pfander, B.; Moldovan, G. L.; Pyrowolakis, G.; Jentsch, S. *Nature* **2002**, *419*, 135–141.

(21) Deng, L.; Wang, C.; Spencer, E.; Yang, L.; Braun, A.; You, J.; Slaughter, C.; Pickart, C.; Chen, Z. *J. Cell* **2000**, *103*, 351–361.

(22) Wang, B.; Matsuoka, S.; Ballif, B. A.; Zhang, D.; Smogorzewska, A.; Gygi, S. P.; Elledge, S. J. *Science* **2007**, *316*, 1194–1198.

(23) Kim, H.; Chen, J. J.; Yu, X. H. *Science* **2007**, *316*, 1202–1205.

(24) Sobhian, B.; Shao, G. Z.; Lilli, D. R.; Culhane, A. C.; Moreau, L. A.; Xia, B.; Livingston, D. M.; Greenberg, R. A. *Science* **2007**, *316*, 1198–1202.

(25) Lewis, M. J.; Saltibus, L. F.; Hau, D. D.; Xiao, W.; Spyropoulos, L. *J. Biomol. NMR* **2006**, *34*, 89–100.

(26) Eddins, M. J.; Carlile, C. M.; Gomez, K. M.; Pickart, C. M.; Wolberger, C. *Nat. Struct. Mol. Biol.* **2006**, *13*, 915–920.

enhancement. Combined with a 10-fold variability in  $K_M$  for substrate binding gives a 1000-fold window in  $k_{\text{cat}}/K_M$ , raising the intriguing possibility that the mechanism underlying the specificity of E2-catalyzed reactions can be determined in part by differences in proficiency among this family of enzymes. The results have broad implications for regulation of the assembly of polyUb chains and importantly attachment of Ub or Ub-like modifiers to substrates through mediators such as E3 Ub ligases. Additionally, the results suggest a mechanism for kinetic control of the ubiquitination of diverse substrates for a given E2 enzyme as well as control of cross talk between pathways regulated by both Ub and Ub-like covalent modifications, such as those involved in postreplicative DNA repair.<sup>20</sup>

## Materials and Methods

**Kinetics of the Mms2–Ubc13 Interaction from NMR Spectroscopy: Line-Shape Analysis.** Protein expression and purification was conducted as previously described.<sup>27</sup> 2D  $^1\text{H}$ – $^{15}\text{N}$  HSQC NMR spectra for the titration of 0.34 mM [ $U$ - $^{15}\text{N}$ ]-Ubc13 with unlabeled Mms2 were collected at 25 °C and 600 MHz. Protein concentration ratios (Ubc13:Mms2) for the titration were 8.3, 4.3, 2.9, 2.1, 1.6, 1.3, 1.1, and 0.9. The NMR sample contained 0.34 mM [ $U$ - $^{15}\text{N}$ ]-Ubc13 in 9:1  $\text{H}_2\text{O}/\text{D}_2\text{O}$ , containing 150 mM HEPES, 75 mM NaCl, 10 mM DTT, 1 mM EDTA, 1 mM DSS (internal chemical shift reference), pH 7.5, in a 5 mm NMR tube. Protein concentrations were determined using the bicinchoninic acid (BCA) assay. The error in protein concentration using the BCA assay is 10%. Line-shape analysis for the titration was conducted using the Bloch–McConnell equations for two-site exchange,<sup>28</sup> adjusted to include the application of a cosine-squared window function. In addition, to account for differential relaxation losses during the INEPT delays, the equations included a 2-fold loss of intensity for the bound state (Mms–Ubc13 complex), given the 2-fold increase in size compared to Mms2 alone. NMR spectra were numerically fit to the frequency domain expression derived from the Bloch–McConnell equations by optimizing the values of  $k_{\text{off}}$ , the bound chemical shift, intensity parameters for individual spectra, and a global intensity parameter. The association rate was  $k_{\text{on}} = k_{\text{off}}/K_D$  with  $K_D = 49$  nM, as previously determined.<sup>29</sup> The error in  $k_{\text{off}}$  was determined by line-shape analysis of the titration at the upper ( $1.1[\text{Ubc13}]_{\text{total}}, 0.9[\text{Mms2}]_n$ ) and lower ( $0.9[\text{Ubc13}]_{\text{total}}, 1.1[\text{Mms2}]_n$ ) error limits for protein concentrations, where  $[\text{Mms2}]_n$  indicates the concentration of Mms2 at the  $n$ th titration point.

**Kinetics of the Mms2–Ubc13 Interaction from NMR Spectroscopy: ZZ-Exchange.** The rate of exchange of  $^{15}\text{N}$  longitudinal magnetization between the free and Ubc13-bound states of Mms2 was characterized using 2D ZZ-exchange spectroscopy.<sup>30,31</sup> 2D  $^1\text{H}$ – $^{15}\text{N}$  HSQC NMR spectra were collected using mixing times of 0, 0.022, 0.044, 0.088, 0.143, 0.187, 0.253, 0.341, 0.528, 0.759, and 1.045 s at 600 MHz. NMR samples contained 350  $\mu\text{L}$  of 0.65 mM [ $U$ - $^{15}\text{N}$ ]-Mms2 with 0.32 mM Ubc13 (2:1 ratio) in a mixed buffer containing 20 mM sodium phosphate, 20 mM TRIS, 150 mM NaCl, 1 mM DTT at pH 7.0 in 9:1  $\text{H}_2\text{O}/\text{D}_2\text{O}$ . The time dependence of the auto- and cross-peak intensities were fit to eq 3 in ref 32, wherein the pseudo-first-order rate constant ( $k_{\text{on}}[\text{Ubc13}]$ ) for ligand binding was employed. The different relaxation properties

for the free and Ubc13-bound states of Mms2 during the INEPT transfers were accounted for by optimization of parameters to adjust the intensities of the auto- and cross-peaks.<sup>32,33</sup> Errors for the kinetic parameters from ZZ-exchange were determined using 500 Monte Carlo trials of the fits using a 10% error in protein concentration, as determined using the BCA assay.  $^{15}\text{N}$ - $R_1$  values for the main chain amides of free and Ubc13-bound Mms2 were collected as previously described; these values were used when fitting the ZZ-exchange data.<sup>34,35</sup>

**Enzyme Assays for Lys63-Linked Ub<sub>2</sub> Synthesis Catalyzed by Mms2–Ubc13.** All proteins other than E1 enzyme and acceptor Ub (purchased from Boston Biochem, Cambridge, MA) were expressed as GST fusion proteins and purified using GST affinity and size-exclusion chromatography, as previously described.<sup>27</sup> The kinetics of polyUb chain formation catalyzed by Mms2–Ubc13 were characterized by analyzing enzyme assays with SDS-PAGE and employing donor Ub site-specifically labeled at the N-terminus with the AlexaFluor 488 probe using maleimide chemistry. Briefly, given that Ub does not contain Cys residues, molecular cloning techniques were used to introduce an N-terminal Cys plus three residues (Leu-Gly-Ser) from Met1 of Ub. On the basis of a recent crystal structure of Mms2/Ubc13 with donor Ub attached to Ubc13 through an oxoester link (PDB ID 2GMD),<sup>26</sup> this location is not expected to interfere with donor Ub interactions with Mms2–Ubc13.

Single-turnover ubiquitination assays were conducted by using E1 to conjugate AlexaFluor 488 labeled Ub (donor Ub) to Ubc13 first at pH 7.3, then quenching the reaction with EDTA. Ub<sub>2</sub> chain synthesis was subsequently initiated by adjusting the pH to the desired value (typically 8.0 but variable for the pH–rate profile) and adding Mms2 and 49–197  $\mu\text{M}$  Ub (acceptor Ub) after quenching the E1 reaction, allowing the kinetics of polyUb chain formation to be followed directly. It should be noted that Ub derived from pGEX-6P1 GST fusion constructs contain a GPLGS cloning artifact at the N-terminus of Ub. Employing acceptor Ub derived from this GST fusion construct in enzyme assays gives  $k_{\text{cat}}$  values that are underestimated by  $\sim 4$ -fold. Therefore, we used wild-type human Ub purchased from Boston Biochem (Cambridge, MA) for enzyme assays. Reaction times for enzyme assays ranged from 2 to 30 min, and typical protein concentrations were 200 nM E1, 8  $\mu\text{M}$  Ubc13, 10  $\mu\text{M}$  Mms2, 10.7  $\mu\text{M}$  Alexa Fluor 488 labeled Ub-K63R, 4 mM  $\text{MgCl}_2$ , and 4 mM ATP in buffer containing 150 mM NaCl and 37 mM BIS-TRIS propane. Enzyme reactions were quenched by flash freezing in liquid nitrogen. Concentrations of Ubc13 and Mms2 in the reaction mixture varied slightly depending on the amount of acceptor Ub added; these differences were accounted for when analyzing enzyme assays. The E1 reaction was quenched with 51 mM EDTA. The fraction of Ubc13 covalently conjugated to AlexaFluor 488 labeled Ub-K63R after reaction with E1 enzyme for 12 min varied between 15% and 60%. Gels were visualized using fluorescence at 517 nm with a Typhoon 9400 Imager (Figure S1, Supporting Information). Protein concentrations were determined by BCA assays; the quantity of Ubc13 that was conjugated to Ub in each assay was determined by using SYPRO Ruby total protein stain following fluorescent imaging of gels.

**Analysis of the Kinetics of Lys63-Linked Ub<sub>2</sub> Synthesis Catalyzed by Mms2–Ubc13.** To analyze enzyme kinetics, we used single-turnover assays to quantify the rate constant for Ub<sub>2</sub> formation catalyzed by human Mms2–Ubc13. The coupled differential equations describing the non-steady-state rate of Ub<sub>2</sub> formation and loss of Ubc13~Ub thioester (Results section) were numerically integrated by setting values for  $k_{\text{cat}}$  and parameters to

- (27) Hau, D. D.; Lewis, M. J.; Saltibus, L. F.; Pastushok, L.; Xiao, W.; Spyropoulos, L. *Biochemistry* **2006**, *45*, 9866–9877.  
 (28) Palmer, A. G.; Kroenke, C. D.; Loria, J. P. *Methods Enzymol.* **2001**, *339*, 204–238.  
 (29) McKenna, S.; Hu, J.; Moraes, T.; Xiao, W.; Ellison, M. J.; Spyropoulos, L. *Biochemistry* **2003**, *42*, 7922–7930.  
 (30) Montelione, G. T.; Wagner, G. J. *Am. Chem. Soc.* **1989**, *111*, 3096–3098.  
 (31) Farrow, N. A.; Zhang, O.; Forman-Kay, J. D.; Kay, L. E. *J. Biomol. NMR* **1994**, *4*, 727–734.  
 (32) Tollinger, M.; Skrynnikov, N. R.; Mulder, F. A. A.; Forman-Kay, J. D.; Kay, L. E. *J. Am. Chem. Soc.* **2001**, *123*, 11341–11352.

- (33) Demers, J. P.; Mittermaier, A. *J. Am. Chem. Soc.* **2009**, *131*, 4355–4367.  
 (34) Farrow, N. A.; Muhandiram, R.; Singer, A. U.; Pascal, S. M.; Kay, C. M.; Gish, G.; Shoelson, S. E.; Pawson, T.; Forman-Kay, J. D.; Kay, L. E. *Biochemistry* **1994**, *33*, 5984–6003.  
 (35) Spyropoulos, L.; Lewis, M. J.; Saltibus, L. F. *Biochemistry* **2005**, *44*, 8770–8781.

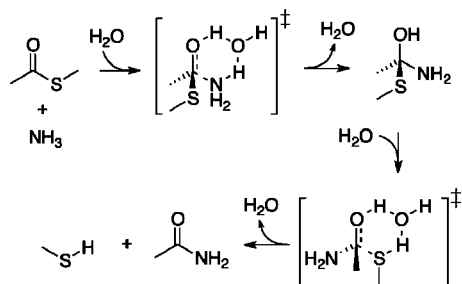


**Figure 1.** Stepwise reaction mechanism for aminolysis of methyl thioacetate.

adjust for total Ub<sub>2</sub> (product) formed and total Ubc13~Ub consumed, specific to each data set. To determine a global  $k_{\text{cat}}$ , values for these parameters were optimized by global minimization of the squared difference between four experimental enzyme assays and theoretical Ub<sub>2</sub> and Ubc13~Ub concentrations using an in-house simulated annealing algorithm. Determination of the pH-rate profile for Mms2~Ubc13 was achieved by conducting enzyme assays at pH values of 7.0, 7.5, 7.75, 8.0, 8.5, and 9.0. The value of  $k_{\text{cat}}$  was numerically optimized for each individual pH as described above. The pH-dependent  $k_{\text{cat}}$  data were fit to the function  $k_{\text{cat}} = (10^{\text{pH}} k_{\text{cat,base}}) / (10^{\text{pH}} + 10^{\text{pK}_a})$ , with  $k_{\text{cat,base}}$  and  $\text{pK}_a$  as adjustable parameters.<sup>12</sup>  $k_{\text{cat,base}}$  is the rate constant corresponding to pH values for which the substrate Lys exists entirely as the neutral form (Lys-NH<sub>2</sub>), with an associated  $\text{pK}_a$ . For the numerical integration and optimization, values for  $k_{\text{on}}$  and  $k_{\text{off}}$  of  $(2.0 \pm 0.6) \times 10^7 \text{ M}^{-1} \text{ s}^{-1}$  and  $600 \pm 200 \text{ s}^{-1}$ , respectively, were used for the interaction of Ub with the Mms2~Ubc13 heterodimer.<sup>29</sup> In addition, we assumed that acceptor and donor Ub molecules do not interact. This latter assumption is reasonable given recent crystal structures and chemical shift data (structures Ub<sub>2</sub>, 2JF5, Mms2~Ubc13~Ub, 2GMI; chemical shifts, ref 27). Furthermore, the kinetics of the Ubc13~Mms2 interaction are included in the numerical integration; these  $k_{\text{on}}$  and  $k_{\text{off}}$  values were determined as described above, with further details in the Results section. The error for the global value of  $k_{\text{cat}}$  and the values of  $k_{\text{cat}}$  from the pH-rate profile were determined using 25 Monte Carlo trials of the fits using a 10% error in the concentrations of Ubc13, Mms2, and wild-type acceptor Ub as well as the errors for the various  $k_{\text{on}}$  and  $k_{\text{off}}$  values for the interaction between Mms2 and Ub, Mms2~Ubc13 and Ub, and between Mms2 and Ubc13.

## Results

**E2 Enzymes Achieve Large Rate Enhancements Compared to the Reaction in Water.** Modulation of the catalytic proficiency [ $(k_{\text{cat}}/K_M)/k_{\text{noncat}}$ ] of E2 enzymes, through modest variations in  $k_{\text{cat}}$ ,  $K_M$ , or both, likely represents a mechanism by which different E2 enzymes achieve different biological outcomes. While there have been numerous measurements of  $k_{\text{cat}}$  and  $K_M$  for E2 enzymes, the catalytic proficiency remains unspecified. To determine the overall rate enhancement achieved by the enzyme, a noncatalyzed rate for thioester aminolysis under physiological conditions needs to be calculated to facilitate comparison to the enzyme-catalyzed rate. The mechanism for thioester aminolysis in water is widely considered to be a nucleophilic acyl substitution reaction (Figure 1).<sup>36,37</sup> The rate equation describing this reaction in aqueous solution and relevant to the reaction catalyzed by E2 enzymes is given by<sup>11</sup>

$$\frac{d[\text{TE}]}{dt} = k_1[\text{TE}][\text{RNH}_2] + k_2[\text{TE}][\text{RNH}_2][\text{OH}^-] \quad (1)$$

(36) Bender, M. L. *J. Am. Chem. Soc.* **1951**, *73*, 1626–1629.

(37) Yang, W.; Drueckhammer, D. G. *Org. Lett.* **2000**, *2*, 4133–4136.

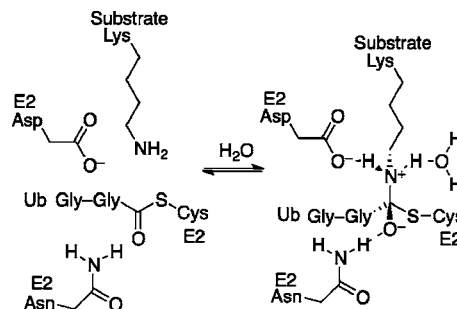


**Figure 2.** First step in a stepwise reaction mechanism for thioester aminolysis catalyzed by E2 enzymes. The transition state is shown on the right. For the serine proteases, the oxyanion is stabilized by two hydrogen bonds, whereas only one such H bond has been identified for E2 enzymes. Proton transfer from the amine to the sulfur (likely facilitated by water), with cleavage of the C–S bond, completes the reaction. Active site E2 residues include a conserved Asn and Cys and an Asp/Glu proximal to the substrate Lys. The C-terminal Gly from Ub or Ubl modifiers is attached to the active site Cys of the E2 through a thioester bond, and Lys from the substrate performs the nucleophilic attack.

where TE is thioester ( $\text{R}'\text{COSR}''$ ),  $k_1 = 0.015 \text{ M}^{-1} \text{ s}^{-1}$ , and  $k_2 = 13.6 \text{ M}^{-2} \text{ s}^{-1}$ . To facilitate comparison to the enzyme-catalyzed reaction, terms involving  $\text{OH}^-$ -catalyzed hydrolysis of thioester and  $\text{RNH}_2$ -catalyzed thioester aminolysis are excluded. The biological reaction occurs at an intracellular pH of 7.2 and 37 °C. For a thioester concentration of 10  $\mu\text{M}$ , an estimate for the maximum intracellular concentration of thioester-charged E2 enzyme,<sup>38</sup> and a total amine concentration ( $\text{RNH}_2$  and  $\text{RNH}_3^+$ ) of 20  $\mu\text{M}$ , an estimate for the upper limit for the intracellular concentration of Ub,<sup>39,40</sup> eq 1 gives a rate of reaction of  $7.7 \times 10^{-15} \text{ M s}^{-1}$  (pH 7.5 to facilitate comparison to the enzyme reaction). At pH 7.5, the  $\text{RNH}_3^+:\text{RNH}_2$  ratio is  $\sim 1100$ , for an amine  $\text{pK}_a$  of 10.54, using the equation

$$[\text{RNH}_2] = \frac{10^{\text{pH}}[\text{RNH}_3^+ + \text{RNH}_2]}{(10^{\text{pH}} + 10^{\text{pK}_a})} \quad (2)$$

To approximate the rate enhancement due to enzyme, we use for comparison the reaction catalyzed by the E2 Ubc9, with the substrate GST-RanGAP1 (an E2 with the largest known  $k_{\text{cat}}$ ).<sup>12</sup> We assume that the mechanism in the enzyme is similar to that in water and given by the scheme in Figure 2. It is typical to analyze the kinetics of E2-catalyzed reactions using the Michaelis–Menten equation under the assumption of steady-state kinetics<sup>41</sup>

$$v_i = \frac{d[\text{P}]}{dt} = \frac{[E_0][\text{S}]k_{\text{cat}}}{K_M + [\text{S}]} \quad (3)$$

for the enzymatic reaction

(38) Siepmann, T. J.; Bohnsack, R. N.; Tokgoz, Z.; Baboshina, O. V.; Haas, A. L. *J. Biol. Chem.* **2003**, *278*, 9448–9457.

(39) Haas, A. L.; Bright, P. M. *J. Biol. Chem.* **1985**, *260*, 2464–2473.

(40) Hofmann, R. M.; Pickart, C. M. *J. Biol. Chem.* **2001**, *276*, 27936–27943.

(41) Fersht, A. *Structure and mechanism in protein science: A guide to enzyme catalysis and protein folding*; W. H. Freeman: New York, 1999.

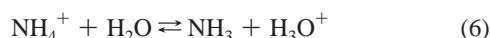


where  $\nu_i$  is the initial rate, P is the product,  $E_0$  is the total enzyme concentration, S is substrate, and  $K_M$  is given by

$$K_M = \frac{k_{\text{off}} + k_{\text{cat}}}{k_{\text{on}}} \quad (5)$$

$K_M$  is approximately equal to  $K_D$ , the dissociation constant for the enzyme substrate complex, under the conditions  $k_{\text{cat}} \ll k_{\text{off}}$ . For the E2 Ubc9, with the substrate GST-RanGAP1, using Michaelis–Menten kinetics (eq 3) gives values of  $k_{\text{cat}} = 0.66 \text{ s}^{-1}$  and  $K_M = 2.9 \mu\text{M}$ .<sup>12</sup> Using these values with an enzyme concentration of  $10 \mu\text{M}$  (thioester) and a substrate concentration of  $20 \mu\text{M}$  in eq 3 gives a reaction rate of  $5.8 \times 10^{-6} \text{ M s}^{-1}$ . Thus, the enzymatic rate enhancement for these conditions is  $7.5 \times 10^8$ . Determination of the catalytic proficiency requires an understanding of how the activation barrier for the reaction in water is reduced in the enzyme active site; this is discussed in more detail in the subsequent sections.

**Overall Activation Barrier for the E2-Catalyzed Reaction Is Smaller Compared to the Reaction in Water.** Numerous computational studies for enzyme reactions indicate that complementary electrostatic interactions between the charged transition state and the active site residues leads to a substantial reduction in the activation barrier for a reaction in an enzyme compared to the reaction within a water cage, that is,  $\Delta\Delta G_{\text{cat}}^\ddagger = \Delta G_{\text{cat}}^\ddagger - \Delta G_{\text{cage}}^\ddagger < 0$ .<sup>14</sup> The first step of the thioester aminolysis reaction involves a proton transfer step from  $\text{NH}_4^+$  or lysine  $\text{NH}_3^+$  to a water molecule



The free energy in solution is given by<sup>42</sup>

$$\Delta G_{\text{PT}}^{\text{S}} = 2.3RT\{\text{p}K_{\text{a}}(\text{NH}_4^+) - \text{p}K_{\text{a}}(\text{H}_3\text{O}^+)\} \quad (7)$$

where  $R$  is the gas constant and  $T$  is the temperature. Using  $\text{p}K_{\text{a}}(\text{NH}_4^+) = 10.54$ , corresponding to the  $\text{p}K_{\text{a}}$  for lysine, and  $\text{p}K_{\text{a}}(\text{H}_3\text{O}^+) = -1$  in eq 7 gives  $\Delta G_{\text{PT}}^{\text{S}} = 15.7 \text{ kcal mol}^{-1}$  for the proton transfer step in water.

For the second step of the reaction, the nucleophilic attack of ammonia on the thioester carbonyl, the rate constant in eq 1 ( $k_2 = 13.6 \text{ M}^{-2} \text{ s}^{-1}$ ) can be used to calculate an activation barrier using transition state theory (TST). The rate constant for a chemical reaction is given by<sup>14,15</sup>

$$k = \kappa k_{\text{TST}} = \kappa \left( \frac{k_{\text{B}}T}{h} \right) \exp \left[ -\frac{\Delta G^\ddagger}{RT} \right] \quad (8)$$

where  $\kappa$  is the transmission coefficient,  $R$ ,  $k_{\text{B}}$ , and  $h$  are the gas, Boltzmann, and Planck constants, respectively,  $T$  is temperature, and  $\Delta G^\ddagger$  is the free energy functional evaluated at the reaction coordinate value for the transition state at standard state concentration. Assuming that the transmission coefficient is  $\sim 1$ , solving for  $\Delta G^\ddagger$  gives the activation barrier in water ( $T = 25.6 \text{ }^\circ\text{C}$ ),  $\Delta G_{\text{w}}^\ddagger = 15.9 \text{ kcal mol}^{-1}$ . The calculation assumes a single transition state, whereas the overall reaction involves two transition states (Figure 1). However, the largest barrier to the reaction is formation of the first transition state, such that eq 8 should provide a

reasonable estimate for the rate of reaction in water. For example, the relative energy of the first transition state (Figure 1) is calculated to be  $10.9 \text{ kcal}$  in water using electronic structure theory.<sup>37</sup> Correcting this value for the entropic cost of bringing the reactants together in a solvent cage ( $\sim 2.4 \text{ kcal mol}^{-1}$ )<sup>17</sup> gives a theoretical  $\Delta G_{\text{w}}^\ddagger = 13.3 \text{ kcal mol}^{-1}$ , in reasonable agreement with the experimental value of  $15.9 \text{ kcal mol}^{-1}$ . It should be noted, however, that the nature of the model compounds differs between the experimental and the theoretical studies.

To calculate the activation barrier for the reaction catalyzed by E2 enzyme ( $\Delta G_{\text{cat}}^\ddagger$ ), it is reasonable to assume that the transmission coefficient is similar in water and the enzyme, with magnitude  $\sim 1$ .<sup>14</sup> For attachment of the Ub-like modifier SUMO to the substrate GST-RanGAP1 by the E2 Ubc9 (pH 7.5,  $37 \text{ }^\circ\text{C}$ ),  $k_{\text{cat}} = 0.66 \text{ s}^{-1}$ ; thus, eq 8 gives  $\Delta G_{\text{cat}}^\ddagger = 18.4 \text{ kcal mol}^{-1}$  for the overall reaction barrier for Ubc9, an E2 with the largest measured  $k_{\text{cat}}$ .<sup>12</sup> Thus, the reduction in the activation barrier for this enzyme is  $\Delta\Delta G_{\text{cat}}^\ddagger = \Delta G_{\text{cat}}^\ddagger - (\Delta G_{\text{w}}^\ddagger + \Delta G_{\text{PT}}^{\text{S}}) = 18.4 - (15.7 + 15.9) = -13.2 \text{ kcal mol}^{-1}$ . As discussed in further detail below, the contributing factors to  $\Delta\Delta G_{\text{cat}}^\ddagger$  are entropic effects of binding, electrostatic stabilization of the transition state, as well as suppression of the substrate lysine  $\text{p}K_{\text{a}}$  through electrostatic effects.

#### Errors Associated with Measurement of $k_{\text{cat}}$ and $K_M$ for E2 Enzymes Using Steady-State Michaelis–Menten Kinetics.

E2-catalyzed reactions are often studied using steady-state Michaelis–Menten kinetics.<sup>7,12,40,43,44</sup> This approach has often been used to measure relative apparent catalytic rates. However, in a strict sense, the kinetics are non-steady state given that the enzyme, E2 thioester, is consumed during the reaction. To estimate the magnitude of the error associated with the steady-state assumption, we employ the following rate equations for E2-catalyzed reactions, wherein the substrate directly binds E2, to calculate reaction rates

$$\frac{d[\text{E2} \sim \text{Ub}]}{dt} = k_{\text{off,S}}[\text{S} \cdot \text{E2} \sim \text{Ub}] - k_{\text{on,S}}[\text{S}][\text{E2} \sim \text{Ub}] + k_{\text{off,S}}[\text{Ub} \sim \text{S} \cdot \text{E2} \sim \text{Ub}] - k_{\text{on,S}}[\text{Ub} \sim \text{S}][\text{E2} \sim \text{Ub}]$$

$$\frac{d[\text{S} \cdot \text{E2} \sim \text{Ub}]}{dt} = -k_{\text{off,S}}[\text{S} \cdot \text{E2} \sim \text{Ub}] + k_{\text{on,S}}[\text{S}][\text{E2} \sim \text{Ub}] - k_{\text{cat}}[\text{S} \cdot \text{E2} \sim \text{Ub}]$$

$$\frac{d[\text{Ub} \sim \text{S} \cdot \text{E2} \sim \text{Ub}]}{dt} = -k_{\text{off,S}}[\text{Ub} \sim \text{S} \cdot \text{E2} \sim \text{Ub}] + k_{\text{on,S}}[\text{Ub} \sim \text{S}][\text{E2} \sim \text{Ub}]$$

$$\frac{d[\text{E2}]}{dt} = k_{\text{off,S}}[\text{S} \cdot \text{E2}] - k_{\text{on,S}}[\text{S}][\text{E2}] + k_{\text{off,S}}[\text{Ub} \sim \text{S} \cdot \text{E2}] - k_{\text{on,S}}[\text{Ub} \sim \text{S}][\text{E2}]$$

(43) Pickart, C. M.; Haldeman, M. T.; Kasperek, E. M.; Chen, Z. *J. Biol. Chem.* **1992**, *267*, 14418–14423.

(44) Haldeman, M. T.; Xia, G.; Kasperek, E. M.; Pickart, C. M. *Biochemistry* **1997**, *36*, 10526–10537.

(42) Warshel, A. *Biochemistry* **1981**, *20*, 3167–3177.

$$\begin{aligned} \frac{d[S \cdot E2]}{dt} &= -k_{\text{off},S}[S \cdot E2] + k_{\text{on},S}[S][E2] \\ \frac{d[\text{Ub} \sim S \cdot E2]}{dt} &= -k_{\text{off},S}[\text{Ub} \sim S \cdot E2] + \\ & k_{\text{on},S}[\text{Ub} \sim S][E2] + k_{\text{cat}}[S \cdot E2 \sim \text{Ub}] \\ \frac{d[S]}{dt} &= k_{\text{off},S}[S \cdot E2 \sim \text{Ub}] - k_{\text{on},S}[S][E2 \sim \text{Ub}] + \\ & k_{\text{off},S}[S \cdot E2] - k_{\text{on},S}[S][E2] \\ \frac{d[\text{Ub} \sim S]}{dt} &= k_{\text{off},S}[\text{Ub} \sim S \cdot E2 \sim \text{Ub}] - k_{\text{on},S}[\text{Ub} \sim S][E2 \sim \text{Ub}] \\ & + k_{\text{off},S}[\text{Ub} \sim S \cdot E2] - k_{\text{on},S}[\text{Ub} \sim S][E2] \end{aligned} \quad (9)$$

where S is substrate protein,  $k_{\text{on},S}$  and  $k_{\text{off},S}$  are the on and off rates of substrate binding to charged ( $E2 \sim \text{Ub}$ ) and uncharged E2, respectively,  $k_{\text{cat}}$  is the catalytic rate, bullet points indicate a noncovalent interaction, and wavy lines indicate a thioester bond ( $E2 \sim \text{Ub}$ ) or an amide bond for the final attachment of Ub to substrate. The corresponding equilibria for eq 9 are shown in Figure 3. These rate equations can be solved for the concentration of product ( $S \sim \text{Ub}$ ) under a given set of reaction conditions, “true” rate constants, various substrate concentrations, and various times. The product build up for the various substrate concentrations can subsequently be linearly fit to determine simulated initial rates of substrate ubiquitination. These simulated initial rates can then be fit to eq 3 to yield fitted  $k_{\text{cat}}$  and  $K_M$  values. Differences between the true  $k_{\text{cat}}$  and  $K_M$  and the fitted values give the error due to the assumption of steady-state, Michaelis–Menten kinetics. For example, given an initial enzyme concentration ( $E2 \sim \text{Ub}$ , or  $E_0$ ) of 21 nM,  $K_D = k_{\text{off}}/k_{\text{on}} = 2.8 \mu\text{M}$  ( $k_{\text{off}} = 56 \text{ s}^{-1}$ ,  $k_{\text{on}} = 2 \times 10^7 \text{ M}^{-1} \text{ s}^{-1}$ ) for binding of substrate to E2, reaction times of 37, 74, 111, and 148 ms, and a true  $k_{\text{cat}}$  of  $1.0 \text{ s}^{-1}$ , we calculated initial rates of 2.7, 4.7, 6.3, and  $7.7 \text{ nM s}^{-1}$  at substrate concentrations of 0.5, 1.0, 1.5, and  $2.0 \mu\text{M}$ , respectively (Figure 4). Fitting these initial rates to the Michaelis–Menten equation (eq 3) gives a  $k_{\text{cat}}$  of  $0.95 \text{ s}^{-1}$  and a  $K_M$  of  $3.1 \mu\text{M}$ , corresponding to errors of 4% and 17%, respectively, in comparison to the true values (Figure 4). Changing the reaction times to 1, 2, 3, and 4 s gives a  $k_{\text{cat}}$  of  $0.28 \text{ s}^{-1}$  and a  $K_M$  of  $0.8 \mu\text{M}$ , corresponding to errors of 72% and 71%, respectively (Figure 4). This analysis gives a general idea of the accuracy of the steady-state Michaelis–Menten approach to E2-catalyzed reactions where the E2 binds substrate directly. Furthermore, we note that the maximum concentration of substrate must exceed  $K_M$  in order to ensure accuracy for this fitted parameter. To further illustrate these points, Figure 5 shows the error in  $k_{\text{cat}}$  for various values of maximum reaction time ( $t_{\text{max}}$ ) and  $k_{\text{cat}}$  for two types of E2 enzyme: one with tight substrate binding and another with weak substrate binding. Accuracy deteriorates with increasing  $k_{\text{cat}}$  and increasing  $t_{\text{max}}$ , the time over which initial rates are obtained.

For the rate equations of thioester aminolysis catalyzed by E2 enzymes (eq 9), the rate of  $\text{OH}^-$ -catalyzed hydrolysis of thioester was ignored given that it is slow.<sup>11,45</sup> For example, the second-order rate constant at  $26 \text{ }^\circ\text{C}$  is  $k_{\text{OH}} = 0.53 \text{ M}^{-1} \text{ s}^{-1}$ .<sup>11</sup> Thus, at pH 7.5 and  $37 \text{ }^\circ\text{C}$  and with a thioester

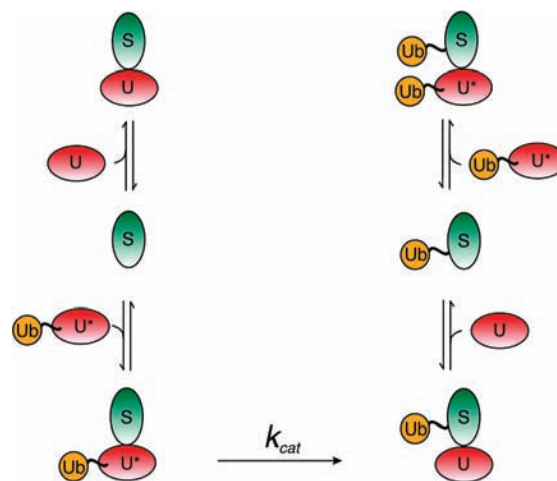


**Figure 3.** Kinetics for the direct ubiquitination of substrates by E2 enzymes. Substrate protein is indicated by an S and shown in green, Ub13 covalently attached to Ub through a thioester bond (charged Ub13) is indicated by  $U^*$  and colored red, uncharged Ub13 is indicated by a U and shown in red, and Ub is colored yellow.

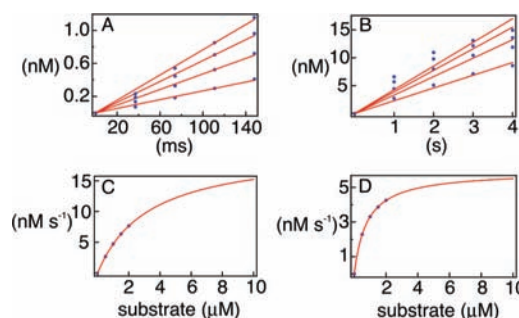


**Figure 4.** Steady-state Michaelis–Menten simulations for direct ubiquitination of substrates by E2 enzymes. Initial rates were determined from linear fits of short time scale (A) and long time scale reactions (B). The initial rates were fit to the Michaelis–Menten equation for the short (C) and long (D) time scale reactions.

concentration of  $15 \mu\text{M}$ , the rate of hydrolysis is given by  $k_{\text{OH}}[\text{TE}][\text{OH}^-] = 7 \times 10^{-12} \text{ M s}^{-1}$ . This value compares favorably with the first-order rate of hydrolysis for the Ub13 $\sim$ SUMO thioester,  $k = (5 \pm 3) \times 10^{-5} \text{ s}^{-1}$ .<sup>45</sup> This gives a rate of  $8 \times 10^{-10} \text{ M s}^{-1}$  at pH 7.4,  $37 \text{ }^\circ\text{C}$ , and with a thioester concentration of  $15 \mu\text{M}$ .

**Non-Steady-State Kinetics Underlying Assembly of Lys63-Linked polyUb Chains.** Mms2 and Ub13 form a noncovalent enzyme complex, and the kinetics of this interaction are not accounted for in the basic Michaelis–Menten enzymatic reaction (eqs 3–5). To derive the rate equations for the chemical reaction catalyzed by Mms2–Ub13, the starting point is a description of the equilibria for the interaction of Mms2 and Ub13 with each other and Ub (Figure 6).

(45) Song, J.; Wang, J.; Jozwiak, A. A.; Hu, W.; Swiderski, P. M.; Chen, Y. *Protein Sci.* **2009**, *18*, 2492–2499.

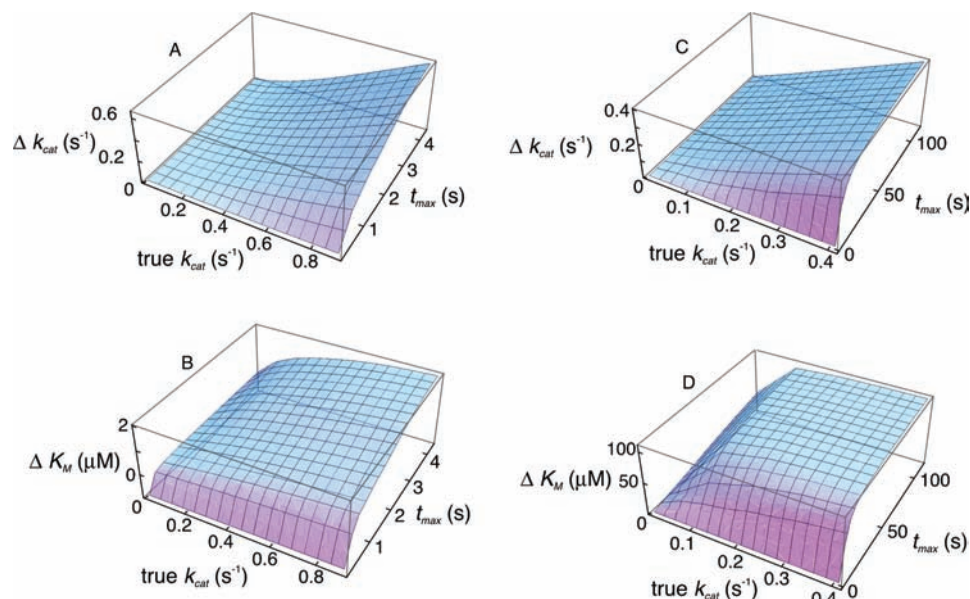


**Figure 5.** Errors associated with the assumption of steady-state Michaelis–Menten kinetics for E2-catalyzed reactions.  $\Delta k_{\text{cat}} = \text{true } k_{\text{cat}} - \text{fitted } k_{\text{cat}}$ ,  $\Delta K_{\text{M}} = \text{true } K_{\text{D}} - \text{fitted } K_{\text{M}}$ , and  $t_{\text{max}}$  is the maximum time over which initial rates were taken in steps of  $t_{\text{max}}/4$  (Figure 4A and 4B). The initial enzyme concentration,  $E_0$  or  $E_2 \sim \text{Ub}$ , was 21 nM, the  $K_{\text{D}}$  for substrate binding to E2 was 2.8  $\mu\text{M}$  ( $k_{\text{off}} = 56 \text{ s}^{-1}$ ,  $k_{\text{on}} = 2 \times 10^7 \text{ M}^{-1} \text{ s}^{-1}$ ), the substrate concentrations were 0.5, 1.0, 1.5, and 2.0  $\mu\text{M}$  for A and B, whereas in C and D  $E_0$  was 21 nM, the  $K_{\text{D}}$  for substrate binding to E2 was 110  $\mu\text{M}$  ( $k_{\text{off}} = 2200 \text{ s}^{-1}$ ,  $k_{\text{on}} = 2 \times 10^7 \text{ M}^{-1} \text{ s}^{-1}$ ), and the substrate concentrations were 0–400  $\mu\text{M}$  in steps of 10  $\mu\text{M}$ . Inclusion of product (ubiquitinated substrate) binding to E2 or  $E_2 \sim \text{Ub}$  in the rate equations has a negligible effect on  $\Delta k_{\text{cat}}$  and  $\Delta K_{\text{M}}$  under the specified conditions and with the assumption that  $K_{\text{D}}$  remains the same as substrate binding.

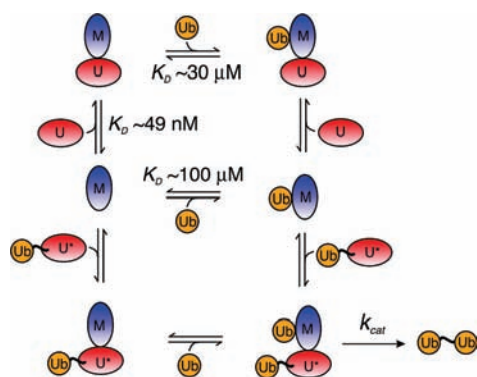
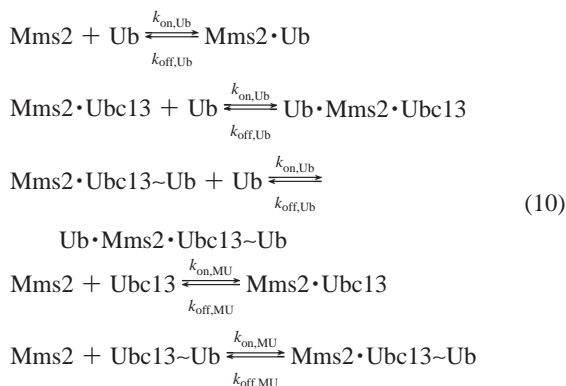


**Figure 6.** Complex kinetics for the Mms2–Ubc13 E2 enzyme system for synthesis of Lys63-linked  $\text{Ub}_2$ . Mms2 is indicated by an M and shown in blue, Ubc13 covalently attached to Ub through a thioester bond (charged Ubc13) is indicated by  $\text{U}^*$  and colored red, uncharged Ubc13 is indicated by a U and shown in red, and Ub is colored yellow.



where bullet points indicate a noncovalent interaction and wavy lines indicate a thioester bond. The  $K_{\text{D}}$  ( $k_{\text{off,Ub}}/k_{\text{on,Ub}}$ )

for binding of substrate or acceptor Ub by Mms2 is 98 and 28  $\mu\text{M}$  for free and Ubc13-bound Mms2, respectively, determined from NMR chemical shift titrations.<sup>29</sup> Given the lack of interaction between donor and substrate Ub molecules,<sup>26,27</sup> we assume that these  $K_{\text{D}}$ s are the same when a donor Ub is covalently attached to the active site cysteine of Ubc13. The  $K_{\text{D}}$  ( $k_{\text{off,MU}}/k_{\text{on,MU}}$ ) for binding of Mms2 and Ubc13 was previously determined to be 49 nM using ITC.<sup>29</sup> We assume that the magnitude of  $K_{\text{D}}$  for this high-affinity interaction remains the same in the presence of Ub covalently attached to Ubc13 or Ub noncovalently bound to Mms2. In addition to these thermodynamic measurements, the rates of protein–protein association/dissociation for the interaction between Mms2 and Ub were previously measured using NMR line-shape analysis.<sup>29</sup> The values of  $k_{\text{on,Ub}}$  and  $k_{\text{off,Ub}}$  were determined to be  $(2.0 \pm 0.5) \times 10^7 \text{ M}^{-1} \text{ s}^{-1}$  and  $2250 \pm 500 \text{ s}^{-1}$ , respectively, with an upper limit for  $k_{\text{off}}$  of  $600 \pm 200 \text{ s}^{-1}$  for binding of Ub to the Mms2–Ubc13 complex.<sup>29</sup> This upper limit was determined by assuming that  $k_{\text{on}}$  for the interaction of Ub with the Mms2–Ubc13 complex is the same as that for the interaction of Ub with Mms2; the different  $K_{\text{D}}$  values for Mms2–Ub and Mms2–Ubc13–Ub give a decrease in  $k_{\text{off}}$  ( $k_{\text{off}} = k_{\text{on}} \times K_{\text{D}}$ ).

In this study, we determined the kinetics of the interaction between Mms2 and Ubc13 ( $k_{\text{on,MU}}$  and  $k_{\text{off,MU}}$ ) using NMR line-shape analysis and ZZ-exchange (Figure 7). The previously measured  $K_{\text{D}}$  of 49 nM for the interaction of Mms2 with Ubc13 was used in NMR line-shape analysis ( $k_{\text{on}} = k_{\text{off}}/K_{\text{D}}$ ) to yield an optimized  $k_{\text{off}}$  of  $4.4 \text{ s}^{-1}$  for Mms2–Ubc13 binding. Assuming a 10% error on the concentrations of Mms2 and Ubc13 yields upper and lower limits for  $k_{\text{off}}$  of 15 and  $5.8 \times 10^{-10} \text{ s}^{-1}$ , respectively. The lower limit appears physically unrealistic; however, assuming that  $k_{\text{on}}$  is diffusion

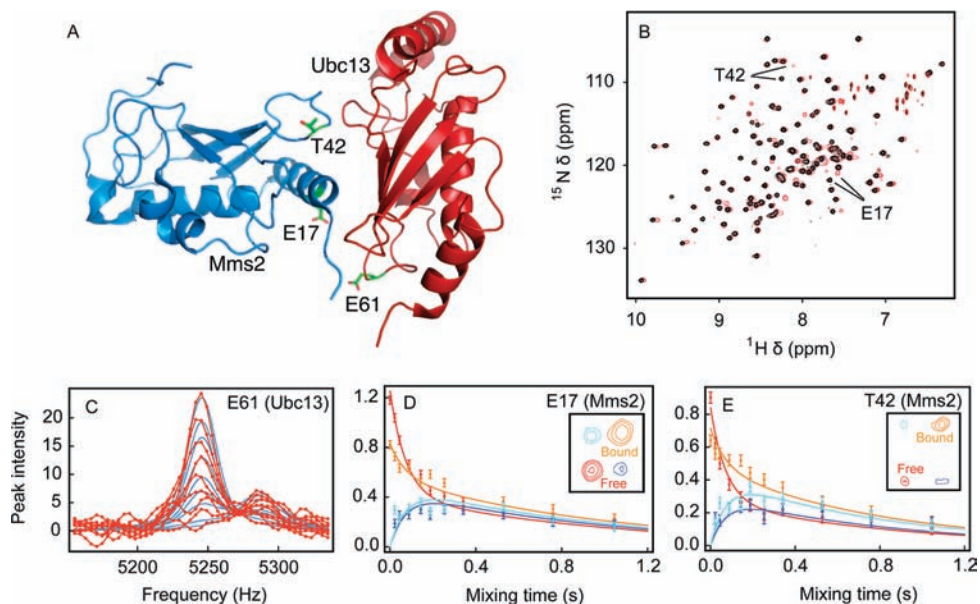


**Figure 7.** NMR measurements for the kinetics of the Mms2–Ubc13 interaction. (A) Structure for the Mms2–Ubc13 complex (PDB ID 1J7D). Residues at the interface undergoing exchange due to the protein–protein interaction are indicated. (B) NMR spectra of free [ $U\text{-}^{15}\text{N}$ ]-Mms2 (black) and [ $U\text{-}^{15}\text{N}$ ]-Mms2 bound to Ubc13 (red). Residues located at the binding interface are indicated. (C) NMR line-shape analysis for the interaction between Mms2 and Ubc13. Experimental data for [ $U\text{-}^{15}\text{N}$ ]-Ubc13 E61  $^1\text{H}^{\text{N}}$  upon titration with Mms2 are shown in red, and simulations are shown in blue.  $^{15}\text{N}$  ZZ-exchange profiles for E17 (D) and T42 (E) from [ $U\text{-}^{15}\text{N}$ ]-Mms2 in a 2:1 ratio with Ubc13. Peak intensity profiles for free and bound peaks are indicated by red and yellow circles, respectively, with the best fits shown as lines. The insets show the ZZ-spectra taken at mixing times of 143 ms for the auto- and cross-peaks of E17 and T42 from free and Ubc13-bound Mms2.

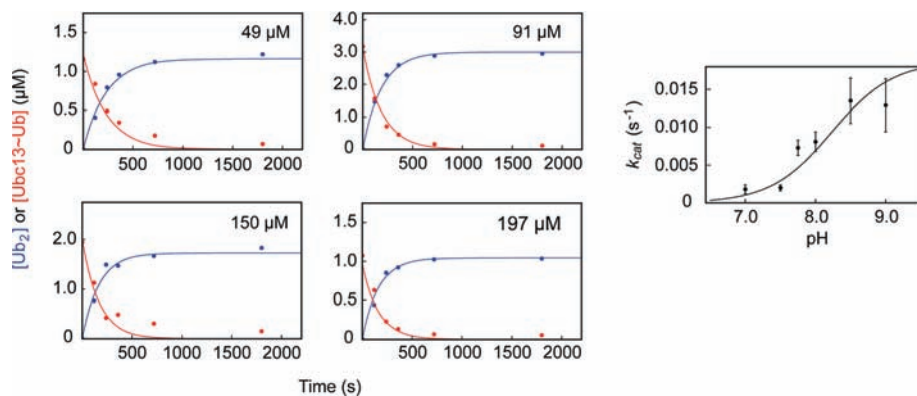


**Figure 8.** (Left) Kinetics of  $\text{Ub}_2$  synthesis catalyzed by the E2 heterodimer Mms2–Ubc13. Enzyme assays involved following the decrease in Ubc13~Ub thioester (red) or the increase in Lys63-linked  $\text{Ub}_2$  (blue). Concentrations of Ub substrate are indicated in the panels for the four separate enzyme assays. Solid lines indicate global fits of the data to the integrated rate equations (eq 11). (Right) pH–rate profile for catalysis of the synthesis of  $\text{Ub}_2$  by Mms2–Ubc13.

controlled with a lower limit of  $10^5 \text{ M}^{-1} \text{ s}^{-1}$ <sup>46</sup> gives a corresponding lower limit for  $k_{\text{off}}$  of  $0.005 \text{ s}^{-1}$ . From the ZZ-exchange measurements, the values for  $k_{\text{on}}$  and  $k_{\text{off}}$  are  $(1.7 \pm 0.5) \times 10^8 \text{ M}^{-1} \text{ s}^{-1}$  and  $4.4 \pm 0.3 \text{ s}^{-1}$  respectively, for the Mms2–Ubc13 interaction.

**Derivation of the Rate Equations Governing Non-Steady-State Kinetics for Assembly of Lys63-Linked polyUb Chains.** Using the reaction scheme for the Mms2–Ubc13 system shown in Figure 6 and eq 10, the time-dependent changes in the concentrations of the various protein species for catalysis of Lys63-linked polyUb chains by the Mms2–Ubc13 heterodimeric E2 enzyme are given by

$$\begin{aligned} \frac{d[\text{Mms2}]}{dt} &= k_{\text{off,Ub}}[\text{Mms2}\cdot\text{Ub}] - k_{\text{on,Ub}}[\text{Mms2}][\text{Ub}] + \\ &\quad k_{\text{off,MU}}[\text{Mms2}\cdot\text{Ubc13}\sim\text{Ub}] \\ &\quad - k_{\text{on,MU}}[\text{Mms2}][\text{Ubc13}\sim\text{Ub}] + k_{\text{off,MU}}[\text{Mms2}\cdot\text{Ubc13}] - \\ &\quad k_{\text{on,MU}}[\text{Mms2}][\text{Ubc13}] \\ \frac{d[\text{Mms2}\cdot\text{Ub}]}{dt} &= k_{\text{on,Ub}}[\text{Mms2}][\text{Ub}] - \\ &\quad k_{\text{off,Ub}}[\text{Mms2}\cdot\text{Ub}] + k_{\text{off,MU}}[\text{Ub}\cdot\text{Mms2}\cdot\text{Ubc13}\sim\text{Ub}] \\ &\quad - k_{\text{on,MU}}[\text{Mms2}\cdot\text{Ub}][\text{Ubc13}\sim\text{Ub}] + \\ &\quad k_{\text{off,MU}}[\text{Ub}\cdot\text{Mms2}\cdot\text{Ubc13}] - \\ &\quad k_{\text{on,MU}}[\text{Mms2}\cdot\text{Ub}][\text{Ubc13}] \end{aligned}$$

(46) Schreiber, G.; Haran, G.; Zhou, H. X. *Chem. Rev.* **2009**, *109*, 839–860.



$$\begin{aligned}
\frac{d[\text{Ubc13}\sim\text{Ub}]}{dt} &= k_{\text{off,MU}}[\text{Ub}\cdot\text{Mms2}\cdot\text{Ubc}\sim\text{13Ub}] - k_{\text{on,MU}}[\text{Mms2}\cdot\text{Ub}][\text{Ubc}\sim\text{13Ub}] \\
&+ k_{\text{off,MU}}[\text{Mms2}\cdot\text{Ubc13}\sim\text{Ub}] - k_{\text{on,MU}}[\text{Mms2}][\text{Ubc13}\sim\text{Ub}] \\
\frac{d[\text{Mms2}\cdot\text{Ubc13}\sim\text{Ub}]}{dt} &= k_{\text{on,MU}}[\text{Mms2}][\text{Ubc}\sim\text{13Ub}] - k_{\text{off,MU}}[\text{Mms2}\cdot\text{Ubc13}\sim\text{Ub}] \\
&- k_{\text{on,Ub}}[\text{Mms2}\cdot\text{Ubc}\sim\text{13Ub}][\text{Ub}] + k_{\text{off,Ub}}[\text{Ub}\cdot\text{Mms2}\cdot\text{Ubc13}\sim\text{Ub}] \\
\frac{d[\text{Ub}\cdot\text{Mms2}\cdot\text{Ubc13}\sim\text{Ub}]}{dt} &= k_{\text{on,MU}}[\text{Mms2}\cdot\text{Ub}][\text{Ubc13}\sim\text{Ub}] - k_{\text{off,MU}}[\text{Ub}\cdot\text{Mms2}\cdot\text{Ubc13Ub}] \\
&+ k_{\text{on,Ub}}[\text{Mms2}\cdot\text{Ubc13}\sim\text{Ub}][\text{Ub}] - k_{\text{off,Ub}}[\text{Ub}\cdot\text{Mms2}\cdot\text{Ubc13}\sim\text{Ub}] \\
&- k_{\text{cat}}[\text{Ub}\cdot\text{Mms2}\cdot\text{Ubc}\sim\text{13Ub}] \\
\frac{d[\text{Mms2}\cdot\text{Ubc13}]}{dt} &= k_{\text{on,MU}}[\text{Mms2}][\text{Ubc13}] - k_{\text{off,MU}}[\text{Mms2}\cdot\text{Ubc13}] - k_{\text{on,Ub}}[\text{Mms2}\cdot\text{Ubc13}][\text{Ub}] \\
&+ k_{\text{off,Ub}}[\text{Ub}\cdot\text{Mms2}\cdot\text{Ubc13}] + k_{\text{cat}}[\text{Ub}\cdot\text{Mms2}\cdot\text{Ubc13}\sim\text{Ub}] \\
\frac{d[\text{Ub}\cdot\text{Mms2}\cdot\text{Ubc13}]}{dt} &= k_{\text{on,MU}}[\text{Ub}\cdot\text{Mms2}][\text{Ubc13}] - k_{\text{off,MU}}[\text{Ub}\cdot\text{Mms2}\cdot\text{Ubc13}] \\
&+ k_{\text{on,Ub}}[\text{Mms2}\cdot\text{Ubc13}][\text{Ub}] - k_{\text{off,Ub}}[\text{Ub}\cdot\text{Mms2}\cdot\text{Ubc13}] \\
\frac{d[\text{Ubc13}]}{dt} &= k_{\text{off,MU}}[\text{Ub}\cdot\text{Mms2}\cdot\text{Ubc13}] - k_{\text{on,MU}}[\text{Mms2}\cdot\text{Ub}][\text{Ubc13}] \\
&+ k_{\text{off,MU}}[\text{Mms2}\cdot\text{Ubc13}] - k_{\text{on,MU}}[\text{Mms2}][\text{Ubc13}] \\
\frac{d[\text{Ub}]}{dt} &= k_{\text{off,Ub}}[\text{Mms2}\cdot\text{Ub}] - k_{\text{on,Ub}}[\text{Mms2}][\text{Ub}] + k_{\text{off,Ub}}[\text{Ub}\cdot\text{Mms2}\cdot\text{Ubc13}\sim\text{Ub}] \\
&- k_{\text{on,Ub}}[\text{Ub}][\text{Mms2}\cdot\text{Ubc13}\sim\text{Ub}] + k_{\text{off,Ub}}[\text{Ub}\cdot\text{Mms2}\cdot\text{Ubc13}] \\
&- k_{\text{on,Ub}}[\text{Mms2}\cdot\text{Ubc13}][\text{Ub}] \\
\frac{d[\text{Ub}_2]}{dt} &= k_{\text{cat}}[\text{Ub}\cdot\text{Mms2}\cdot\text{Ubc13}\sim\text{Ub}]
\end{aligned}
\tag{11}$$

where the bullet points indicate a noncovalent interaction and the wavy lines indicate a thioester bond for E2~Ub or an amide bond for Ub<sub>2</sub>. In principle, an analytical solution for these coupled differential equations can be used to obtain expressions for the concentrations of the various protein species, which can then be used to fit experimental data. However, an analytical solution was not possible; thus, analysis of the kinetics was accomplished by numerical integration of the rate equations after choosing a value for  $k_{\text{cat}}$  and including experimentally determined values for  $k_{\text{on,MU}}$ ,  $k_{\text{off,MU}}$ ,  $k_{\text{on,Ub}}$ , and  $k_{\text{off,Ub}}$  to obtain theoretical protein (Ub<sub>2</sub> and total Ubc13~Ub) concentrations. This procedure was repeated by varying the value of  $k_{\text{cat}}$  using a simulated annealing algorithm to minimize the sum of the squared differences between theoretical and experimental protein concentrations, giving a rate for the chemical step of  $0.007 \pm 0.001$  and  $0.0020 \pm 0.0004 \text{ s}^{-1}$  at pH 8.0 and 7.5, respectively (Figures 8 and 9). Additionally, we measured  $k_{\text{cat}}$  at various pH values for the reaction to determine a  $\Delta\text{p}K_{\text{a}}$  of  $-2.3 \pm 0.1$  for the substrate Lys of acceptor Ub (Figure 8).

## Discussion

**Activation Barrier for the E2-Catalyzed Reaction Is Substantially Reduced Compared to the Reaction in Water.** E2 enzymes are involved in the regulation of a myriad of cellular processes ranging from trafficking, to protein degradation, the DNA damage response, control of the cell cycle, and DNA repair.<sup>3</sup> One of the central questions regarding E2 enzyme activity is whether biological diversity can be achieved through variability in chemical mechanism. Thus, the problem to be addressed is identification of the fundamental source for the catalytic power of these enzymes. This is established by

assuming that the reaction carried out by enzyme follows a mechanism similar to that in water; for bimolecular reactions, the second-order rate constant in water is compared to the enzyme-catalyzed rate.<sup>9,10</sup> However, such comparisons can be complicated as a result of different reaction conditions, the nature of the model compounds with respect to biological substrates, and complex kinetics in enzyme-catalyzed multi-substrate reactions.<sup>47</sup> For reactions involving model compounds relevant to the chemistry of ubiquitination, kinetic studies of aminolysis of thioester bonds in water reveal that the reaction depends on pH and amine concentration and is catalyzed by OH<sup>-</sup>.<sup>11</sup> From the rate constant reported in this early work ( $k_2$  in eq 1) and the free energy of proton transfer from ammonia to water (eq 7), the total activation barrier is  $\Delta G_{\text{w}}^{\ddagger} \approx 31.6 \text{ kcal mol}^{-1}$  with a corresponding  $k_{\text{noncat}} \approx 3.5 \times 10^{-10} \text{ s}^{-1}$  (eq 8). For the SUMO-GST-RanGAP1-Ubc9 reaction, the apparent  $k_{\text{cat}}$  is  $0.66 \text{ s}^{-1}$ <sup>12</sup> (one of the largest  $k_{\text{cat}}$  values for E2 enzymes), giving  $k_{\text{cat}}/k_{\text{noncat}} = 1.9 \times 10^9$ , with a catalytic proficiency ( $k_{\text{cat}}/K_{\text{M}}/k_{\text{noncat}}$ )  $6.5 \times 10^{14} \text{ M}^{-1}$  at pH 7.5 and 37 °C. Thus, E2 enzymes provide a substantial enhancement to the rate of thioester aminolysis that occurs in biological systems insofar as the reaction between *p*-nitrothiolbenzoate and *n*-butylamine is representative of the biological reaction. For Ubc9, there is variability in  $k_{\text{cat}}$  for different substrates. In comparison to the reaction with GST-RanGAP1,  $k_{\text{cat}}$  is 0.021 and 0.027 s<sup>-1</sup> (pH 7.5 and 37 °C) for the substrates p53 (C-terminal tetramerization domain) and GST-PML, respectively, determined using steady-

(47) Frey, P. A.; Hegeman, A. D. *Enzymatic reaction mechanisms*; Oxford University Press: Oxford, New York, 2007.

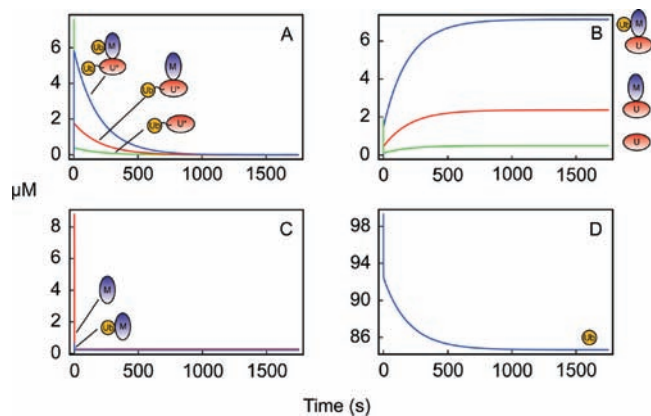


**Figure 9.** Theoretical curves for the kinetics of Ub<sub>2</sub> synthesis catalyzed by Mms2-Ubc13. (A) Concentrations of various Ubc13~Ub thioester or “charged” species: Mms2-Ubc13~Ub (red), Ub-Mms2-Ubc13~Ub (blue), Ubc13~Ub (green). (B) Concentrations of various “uncharged” Ubc13 species: Mms2-Ubc13 (red), Ub-Mms2-Ubc13 (blue), Ubc13 (green). (C) Concentrations of various Mms2 species: free Mms2 (red), Mms2-Ub (blue). (D) Concentration of free Ub. Curves were generated from global fitting of enzyme assays to the integrated rate equations (eq 11) with the following parameters:  $k_{\text{cat}} = 0.007 \text{ s}^{-1}$ ,  $k_{\text{on}} = 2 \times 10^7 \text{ M}^{-1} \text{ s}^{-1}$  and  $k_{\text{off}} = 2250 \text{ s}^{-1}$  for Ub binding to Mms2,  $k_{\text{on}} = 2 \times 10^7 \text{ M}^{-1} \text{ s}^{-1}$  and  $k_{\text{off}} = 560 \text{ s}^{-1}$  for Ub binding to the Mms2-Ubc13 complex,  $k_{\text{on}} = 1.7 \times 10^8 \text{ M}^{-1} \text{ s}^{-1}$  and  $k_{\text{off}} = 4.4 \text{ s}^{-1}$  for Ubc13 binding to Mms2, the concentration of Ub substrate was  $100 \mu\text{M}$ , the total concentration of Mms2 and Ubc13 was  $10 \mu\text{M}$  each, and the total concentration of thioester charged Ubc13 was 80% of the total Ubc13 concentration.

state (p53) and non-steady-state (GST-PML) approaches.<sup>12,48</sup> The rate enhancement for these substrates is  $(6-8) \times 10^7$ , with a catalytic proficiency of  $(0.9-15) \times 10^{11} \text{ M}^{-1}$ . Thus, the catalytic proficiency of E2 enzymes is modest, occurring at the lower end of the spectrum in comparison to a number of other enzymes.<sup>10</sup> In comparison,  $k_{\text{cat}}/k_{\text{noncat}}$  is  $5.7 \times 10^6$  for the Mms2-Ubc13 holoenzyme at pH 7.5 and 37 °C. This enhancement corresponds to a  $\Delta\Delta G_{\text{cat}}^{\ddagger}$  of  $-9.6 \text{ kcal mol}^{-1}$  and a catalytic proficiency of  $1.8 \times 10^{11} \text{ M}^{-1}$ . The  $k_{\text{cat}}$  value for Mms2-Ubc13 at pH 7.5 differs ~14-fold compared to the rate of attachment of SUMO to the protein substrate GST-PML, catalyzed by the E2 Ubc9 ( $k_{\text{cat}} \approx 0.027 \text{ s}^{-1}$ , pH 7.5 and 37 °C).<sup>48</sup> Importantly, the kinetics for the GST-PML/Ubc9 and Ub/Mms2-Ubc13 reactions are directly comparable as they are the only E2-catalyzed reactions analyzed using appropriate non-steady-state approaches.

**Suppression of the Substrate Lysine  $pK_{\text{a}}$  Provides Only Part of the Reduction to the Activation Barrier for the Enzyme-Catalyzed Reaction Compared to the Reaction in Water.** The simplest mechanism to account for the catalytic function of E2 enzymes involves lowering the  $pK_{\text{a}}$  of the substrate lysine to allow deprotonation and subsequent nucleophilic attack of the thioester carbonyl.<sup>12,27</sup> However, this mechanism must be reconciled with generalizations from computational studies that indicate a key source for the catalytic power of enzymes is electrostatic complementarity within the active site.<sup>14,15</sup> Specifically, for attachment of the Ub-like modifier SUMO to the substrate RanGAP1 by the E2 Ubc9, the pH-rate profile for the reaction indicates that the  $pK_{\text{a}}$  of the substrate lysine is decreased by  $-4.1$  units.<sup>12</sup> This magnitude of  $\Delta pK_{\text{a}}$  corresponds to a decrease in the free energy of the

proton transfer step from the substrate lysine to water by  $5.6 \text{ kcal mol}^{-1}$  ( $1 \Delta pK = 1.36 \text{ kcal mol}^{-1}$ ) or an ~8000-fold increase in reaction rate using TST (eq 8). Changes in substrate lysine  $pK_{\text{a}}$  compared to the values in water for E2-catalyzed reactions are essentially electrostatic in nature and reflect changes in the solvation of the ionizable side chain between water and the polar environment of the enzyme active site (eq 13 in ref 49, for example).

For Mms2-Ubc13 and Ubc9,  $\Delta pK_{\text{a}}$  shifts of  $-2.6$  and  $-4.1$  units, respectively, provide maximum contributions to the catalytic rate enhancement of ~200- and ~8000-fold (or 3.2 and  $5.6 \text{ kcal mol}^{-1}$  to  $\Delta\Delta G_{\text{cat}}^{\ddagger}$ ). Thus, suppression of substrate lysine  $pK_{\text{a}}$  represents only part of the total  $\Delta\Delta G_{\text{cat}}^{\ddagger}$  values of  $-9.6$  and  $-13.2 \text{ kcal mol}^{-1}$  for Mms2-Ubc13 and Ubc9, respectively.

**Electrostatic Complementarity and Entropic Effects Play Roles in Reducing the Activation Barrier for the Enzyme-Catalyzed Reaction in Comparison to the Reaction in Water.** In addition to substrate lysine  $pK_{\text{a}}$  suppression, entropic effects of substrate binding<sup>16</sup> and electrostatic complementarity<sup>14</sup> provide additional contributions to  $\Delta\Delta G_{\text{cat}}^{\ddagger}$  for E2 enzymes. Recently, computational studies for a number of enzyme-catalyzed reactions have led to the generalization that enzymes employ electrostatic interactions to stabilize transition states and/or intermediates; the barrier to a reaction is lowered by electrostatic effects from the preorganized, polar environment of the enzyme active site.<sup>14,15</sup> It has been argued that the free energy of binding two reactants can pay for the entropic cost of forming a transition state,<sup>16</sup> and this mechanism was considered to be a major catalytic effect in enzymes. More recent views do not consider this mechanism to be as effective as electrostatic complementarity.<sup>17,50</sup> For example, it is estimated that entropic effects may contribute only  $2.5 \text{ kcal mol}^{-1}$  to catalytic rate enhancement for the enzymatic hydrolysis of a dipeptide using molecular dynamics simulations.<sup>17</sup> Furthermore, small molecule catalysts that exploit entropy effects do not reach the efficiency of enzymes,<sup>51</sup> whereas small molecule catalysts designed to exploit electrostatic complementarity in reduced polarity solvent produce astounding rate accelerations.<sup>52</sup>

With respect to the reaction catalyzed by E2 enzymes, computational studies for small molecules using ab initio electronic structure theory have been employed to model the chemical mechanism.<sup>37,53</sup> The key features of the reaction indicate that catalysis by water facilitates proton transfer from the nucleophilic amine to the thioester carbonyl oxygen and finally the thioester sulfur, proceeding through two transition states and a tetrahedral intermediate. Indeed, elegant isotope exchange experiments are regarded as definitive proof of the existence of the tetrahedral intermediate and the validity of this mechanism.<sup>36,54</sup> From the computational studies, the largest barrier to the reaction involves formation of the first tetrahedral transition state. For the uncatalyzed reaction in water, the charged transition state is stabilized by a water

(48) Tatham, M. H.; Chen, Y.; Hay, R. T. *Biochemistry* **2003**, *42*, 3168-3179.

(49) Kamerlin, S. C. L.; Haranczyk, M.; Warshel, A. *J. Phys. Chem. B* **2009**, *113*, 1253-1272.

(50) Bruce, T. C. *Chem. Rev.* **2006**, *106*, 3119-3139.

(51) Hammes, G. G. *J. Biol. Chem.* **2008**, *283*, 22337-22346.

(52) Neverov, A. A.; Lu, Z. L.; Maxwell, C. I.; Mohamed, M. F.; White, C. J.; Tsang, J. S.; Brown, R. S. *J. Am. Chem. Soc.* **2006**, *128*, 16398-16405.

(53) Yang, W.; Drueckhammer, D. G. *J. Am. Chem. Soc.* **2001**, *123*, 11004-11009.

(54) Bender, M. L.; Kemp, K. C. *J. Am. Chem. Soc.* **1957**, *79*, 111-116.

molecule that bridges opposite charges (Figure 1). For E2 enzymes, mutational studies have led to the suggestion that stabilization of the oxyanion transition state occurs through a conserved Asn.<sup>55</sup> Furthermore, it is likely that an active site Asp residue stabilizes the developing positive charge on the attacking lysine. Stabilization of this transition state in the enzyme active site by hydrogen bonding to the oxyanion and complementing the developing positive charge on the nucleophilic lysine nitrogen may play an important role in the catalytic power of E2 enzymes such as Ubc9 and Ubc13 (Figure 2). Indeed, mutation of a number of charged residues surrounding the substrate lysine in Ubc9 and Ubc13 have been shown to lead to qualitative reductions in the catalytic rate.<sup>12,26,56</sup> These observations are consistent with a key role for electrostatic complementarity in the function of E2 enzymes. Combining entropic effects and  $pK_a$  suppression gives estimates for  $\Delta\Delta G_{\text{cat}}^\ddagger$  of  $-5.7$  and  $-8.1$  kcal mol<sup>-1</sup> for Mms2–Ubc13 and Ubc9, respectively; underestimates in comparison to the observed values of  $-9.6$  and  $-13.2$  kcal mol<sup>-1</sup>, these values indicate that electrostatic stabilization of the transition state for E2 enzymes contributes an additional 4–5 kcal mol<sup>-1</sup> of stabilization or a 2000–3000-fold rate enhancement. Variations in  $k_{\text{cat}}$  due to differences in electrostatic effects such as  $pK_a$  suppression and/or transition state stabilization represent a reasonable molecular basis for the observation that a 10-fold difference in the rate of attachment for the first Ub to a substrate has a large influence on the subsequent fraction of substrate that develops polyUb chains long enough to signal for degradation by the proteasome.<sup>8</sup>

**Steady-State Approaches for Determining  $k_{\text{cat}}$  and  $K_M$  for E3-Mediated Attachment of Ub to Substrates.** Determination of apparent  $k_{\text{cat}}$  and  $K_M$  values using the steady-state assumption with Michaelis–Menten kinetics is potentially inaccurate for kinetically complicated reactions such as E3-mediated transfer of Ub to substrates wherein both E2 and substrate bind E3. In particular, the weaker an E3 binds substrate, the greater the inaccuracy, especially for rate measurements at low substrate concentration. This has important consequences for  $k_{\text{cat}}$  measurements of E2 catalytic activity in the presence of E3s, given that these ubiquitin ligases bind their cognate E2s weakly, with micromolar dissociation constants. The effect of weak binding between Mms2 and Ubc13 or an analogous E3–E2 interaction will lead to apparent  $k_{\text{cat}}$  values that are lower than the true  $k_{\text{cat}}$  (Figure 10). For E2 enzymes that can directly bind substrate, these apparent values can potentially allow for relative comparisons between different substrates, such as attachment of the Ub-like modifier SUMO to p53 and GST-RanGAP1 by the E2 Ubc9.<sup>12</sup> However, as shown in Figure 5, the inaccuracy for  $k_{\text{cat}}$  and  $K_M$  increases as  $k_{\text{cat}}$  increases. If initial rates are determined by linear fitting of kinetic data and subsequently analyzed using the Michaelis–Menten equation, care must be taken to ensure that reactions with larger  $k_{\text{cat}}$  values (0.05 s<sup>-1</sup>) are rapidly sampled on the millisecond time scale. In addition, the rates of direct substrate modification catalyzed by E2 can be enhanced by E3 (E3:E2 Nup358:

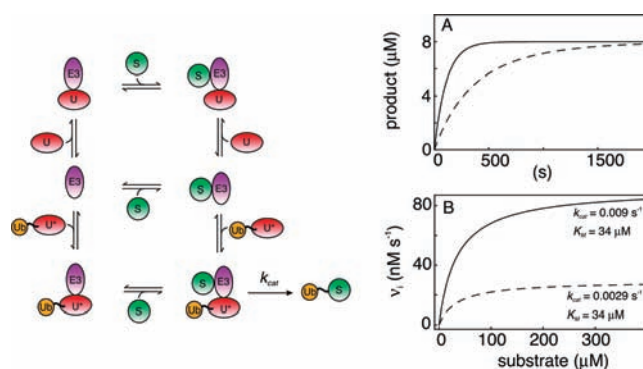


**Figure 10.** E3-mediated substrate ubiquitination by E2 enzymes is shown in the left panel and is essentially the same as the reaction scheme for catalysis of the synthesis of Ub<sub>2</sub> by Mms2–Ubc13 (Figure 6). In the right panel, the rate equations (eq 11) for catalysis of the synthesis of Ub<sub>2</sub> by Mms2–Ubc13 are applied to the E3-mediated formation of ubiquitinated substrate. (A) The solid curve shows the theoretical dependence of the rate of formation of product (substrate~Ub) on the strength of the E2–E3 interaction for  $k_{\text{cat}} = 0.01$  s<sup>-1</sup> and  $K_D = 33$  nM for the E3–E2 interaction ( $k_{\text{on}} = 1.5 \times 10^8$  M<sup>-1</sup> s<sup>-1</sup> and  $k_{\text{off}} = 5$  s<sup>-1</sup>), whereas the dashed curve illustrates substrate~Ub formation upon increasing  $K_D$  to 17 μM ( $k_{\text{on}} = 1.5 \times 10^8$  M<sup>-1</sup> s<sup>-1</sup> and  $k_{\text{off}} = 2500$  s<sup>-1</sup>). The  $K_D$  for the E3–substrate interaction was 30 μM ( $k_{\text{on}} = 2.0 \times 10^7$  M<sup>-1</sup> s<sup>-1</sup> and  $k_{\text{off}} = 300$  s<sup>-1</sup>). (B) Analysis of product build-up under the assumption of steady-state Michaelis–Menten kinetics gives a 3-fold underestimate for  $k_{\text{cat}}$  using an E3–E2  $K_D$  of 17 μM (dashed curve) compared to a  $K_D$  of 33 nM (solid curve). Simulated initial rates were calculated in a similar fashion as those for direct ubiquitination of substrates (Results and Figure 4A), with  $t_{\text{max}} = 10$  s.

Ubc9, with substrate RanBP2),<sup>57</sup> and the complex kinetics for this multisubstrate reaction will give rise to inaccurate apparent kinetic parameters under the assumption of simpler kinetic schemes, as discussed above.

## Conclusion

E2 enzymes play crucial roles in regulating a wide variety of life processes by catalyzing the covalent addition of Ub or Ub-like modifiers to target proteins, thereby modifying the function of the target or signaling for its degradation. Thus, it is important to determine if the biological outcome of ubiquitination can be regulated by variations in the chemical mechanism for different E2 enzymes, as manifested in differences in  $k_{\text{cat}}$  and  $K_M$ . We determined that the catalytic proficiency of E2 enzymes is modest  $\sim 10^{11}$ – $10^{14}$  M<sup>-1</sup> with a magnitude for  $\Delta\Delta G_{\text{cat}}^\ddagger$  from  $-10$  to  $-13$  kcal mol<sup>-1</sup>. The factors that contribute to the catalytic enhancement include substrate lysine  $pK_a$  suppression (3–5 kcal mol<sup>-1</sup>), entropic effects ( $\sim 3$  kcal mol<sup>-1</sup>), and electrostatic complementarity (4–5 kcal mol<sup>-1</sup>). A recent kinetic model for substrate polyubiquitination by the E2 Cdc34 in combination with the E3 SCF demonstrates that a 10-fold difference in the rate of attachment of the first Ub to a substrate can give rise to a substantial difference in the fraction of substrate-bearing polyUb chains long enough to be degraded by the proteasome.<sup>8</sup> Such a modest change in rate can be achieved by modest differences in  $k_{\text{cat}}$ ,  $K_M$ , or both. Interestingly, slight changes in any of the mechanisms for catalysis by E2 enzymes can give rise to variations in  $k_{\text{cat}}$  and lead to the  $\sim 1000$ -fold difference in proficiency among this family of enzymes. Tuning of the catalytic proficiency of different E2s or E2–E3 combinations likely plays a key role in determining

(55) Wu, P. Y.; Hanlon, M.; Eddins, M.; Tsui, C.; Rogers, R. S.; Jensen, J. P.; Matunis, M. J.; Weissman, A. M.; Wolberger, C. P.; Pickart, C. M. *EMBO J.* **2003**, *22*, 5241–5250.

(56) VanDemark, A. P.; Hofmann, R. M.; Tsui, C.; Pickart, C. M.; Wolberger, C. *Cell* **2001**, *105*, 711–720.

(57) Reverter, D.; Lima, C. D. *Nature* **2005**, *435*, 687–692.

the specificity and biological function of E2-catalyzed reactions.

**Acknowledgment.** This research was funded by the Canadian Institutes of Health Research (CIHR) and the University of Alberta. We thank the Canadian National High Field NMR Centre (NANUC) for assistance and for use of the facilities. Operation of NANUC is funded by the Natural Science and Engineering Research Council of Canada and the University of Alberta. L.S. is

an Alberta Heritage Foundation for Medical Research (AHFMR) Senior Scholar.

**Supporting Information Available:** SDS-PAGE gel for a representative Ub<sub>2</sub> assay. This material is available free of charge via the Internet at <http://pubs.acs.org>.

JA105267W